Investigating the Effect of Transcutaneous Electroacupuncture Stimulation on EEG Signals using EEGNet and Saliency Maps

T. Vasei[1], H. Gediya[2], M. Ravan[1], A. Santhanakrishnan[1], D. Mayor[3] and T. Steffert[4]

1. Department of Electrical and Computer Engineering, New York Tech, New York, NY, USA
2. Department of Computer Science, New York Tech, New York, NY, USA
3. School of Computer Science, University of Hertfordshire, Hatfield AL10 9AB, UK
4. MindSpire, Napier House, 14-16 Mount Ephraim Rd, Tunbridge Wells TN1 1EE, UK
{tvasei, hgediya, mravan, asanthan}@nyit.edu,
davidmayor@welwynacupuncture.co.uk, tony@qeeg.co.uk

***Abstract*— Interpretation of electroencephalogram (EEG) signals can be complicated by obfuscating artifacts. Artifact detection plays an important role in the observation and analysis of EEG signals. Spatial information contained in the placement of the electrodes can be exploited to accurately detect artifacts. However, when fewer electrodes are used, less spatial information is available, making it harder to detect artifacts. In this study, we investigate the performance of a deep learning algorithm, CNN-LSTM, on several channel configurations. Each configuration was designed to minimize the amount of spatial information lost compared to a standard 22-channel EEG. Systems using a reduced number of channels ranging from 8 to 20 achieved sensitivities between 33% and 37% with false alarms in the range of [38, 50] per 24 hours. False alarms increased dramatically (e.g., over 300 per 24 hours) when the number of channels was further reduced. Baseline performance of a system that used all 22 channels was 39% sensitivity with 23 false alarms. Since the 22-channel system was the only system that included referential channels, the rapid increase in the false alarm rate as the number of channels was reduced underscores the importance of retaining referential channels for artifact reduction. This cautionary result is important because one of the biggest differences between various types of EEGs administered is the type of referential channel used.**

Keywords*— *EEG signal classification, EEGNet, Saliency map, Transcutaneous electroacupuncture stimulation (TEAS).

I. Introduction

Transcutaneous Electrical Acupoint Stimulation (TEAS) merges traditional acupuncture with modern electrical stimulation, offering a non-invasive alternative to manual acupuncture (MA) and electroacupuncture (EA) [1]. TEAS has gained attention for its therapeutic benefits, notably in enhancing postoperative recovery, managing pain, and improving sleep quality [2–4]. TEAS's non-invasive nature reduces infection risk and discomfort, making it suitable for patients with needle phobia or bleeding disorders. Studies have shown its efficacy in neurorehabilitation, chronic pain management, and alleviating chemotherapy-induced peripheral neuropathy [5],[6]. Despite its benefits, the mechanisms through which TEAS influences brain activity remain unclear. Advanced neuroimaging tools such as electroencephalogram (EEG) and functional magnetic resonance imaging (fMRI) have been employed to study acupuncture's effects. Previous research indicates that both low and high-frequency stimulations have distinct analgesic mechanisms [7, 8]. Only one study has applied a deep learning algorithm to TEAS, which employed a hybrid CNN-LSTM model [9].

This study aims to enhance the understanding of TEAS's neurophysiological effects by using EEGNet, a specialized CNN, to accurately classify brain responses to four different TEAS frequencies (2.5, 10, 80, and sham). Building on previous work [9], we introduce a novel phase-based analysis, capturing dynamic brain responses across pre-stimulation, stimulation, and post-stimulation phases. Additionally, saliency maps are used to identify key EEG electrodes, reducing the number needed without sacrificing accuracy, and an analysis of EEG frequency bands (delta, theta, alpha, beta, gamma) reveals their sensitivity to TEAS. These innovations offer both a comprehensive view of brain responses and practical improvements for optimizing therapeutic applications.

II. Methods

II-A. Study Design and Data Collection

The study received ethical approval from the University of Hertfordshire's Health and Human Sciences Ethics Committee, under protocol number HSK/SF/UH/00124. The study involved 48 participants with a diverse range of ages (18 to 69 years) and a mix of sexes (18 male and 30 female). Each session comprised eight 5-minute periods, categorized as Baseline (first slot), Stimulation (second to fifth slots), and Post-stimulation (sixth to eighth slots). TEAS was administered using a charge-balanced Equinox E-T388 stimulator at frequencies of 2.5, 10, 80, or 160 pulses per second (pps), with the 160 pps frequency serving as a 'sham' treatment due to its very low amplitude, which many participants could not detect.The selection of the three TEAS frequencies—2.5, 10, and 80 pps—was based on their common use in clinical practice and existing literature on TEAS [10]. The sequence of stimulation frequencies was semi-randomized among participants to reduce order effects.

EEG data were recorded from 19 electrodes according to the international 10/20 system, with linked ears as the reference and a ground electrode placed anterior to Fz. Custom-fitted Electro Cap International (ECI) caps were used for participant comfort and data quality. The EEG signals were amplified using a Mitsar EEG-202 amplifier and digitized at a sampling rate of 500 Hz. Preprocessing included the removal of noise and artifacts to generate clean EEG datasets for each participant, suitable for further analysis. The EEG periods were divided into five 1-minute segments, each split into two halves. 10-second epochs were extracted from the beginning of each half (at the 0 and 30-second marks). This approach produced ten epochs per period, resulting in a comprehensive dataset for evaluating the effects of the different TEAS frequencies on EEG activity. The Equinox stimulator and the arrangement of sensors and electrodes are depicted, featuring the fingertip photoplethysmography (PPG) sensor, an ECG electrode positioned on the right forearm, and TENS (transcutaneous electrical nerve stimulation) electrodes located at the LI4 (HeGu) acupoint and along the ulnar edge of the hands.

II-B. Data Preprocessing

The EEG data were band-pass filtered between 0.5 and 45 Hz using second-order Butterworth filters to remove noise, including the 50 Hz power line interference. Independent Component Analysis (ICA) was applied using the extended Infomax algorithm [11] to remove artifacts. We used the MNE-Python library, with FastICA and PCA retaining 99% of variance to ensure optimal artifact removal without overfitting. MARA [12] and ICLabel [13] further refined artifact rejection. Epochs with amplitude deviations exceeding ±3 standard deviations were removed [9]. Data were re-referenced using a current source density (CSD) transformation [14]. Each 10-second epoch was divided into 1-second trials, resulting in approximately 4750-4800 trials per stimulation frequency across all slots.

II-C. Applying EEGNet to TEAS Data

We employed EEGNet, a convolutional neural network architecture optimized for EEG-based brain-computer interfaces (BCIs) [15], to classify EEG data recorded during TEAS sessions. EEGNet processes the input through convolutional and pooling layers specifically tailored for EEG signal classification. Figure 1 illustrates the customized EEGNet architecture on TEAS data.

The input layer accepts a 3D matrix of shape (19 electrodes, 500 samples, 1). The first convolutional block applies a 2D convolution across the temporal dimension, followed by depthwise convolution for spatial filtering. Separable convolutions in the second block reduce computational cost. Both blocks use ELU activation, average pooling, and dropout layers to prevent overfitting.

The model was trained using the Adam optimizer with a learning rate of 0.0001. Although the maximum number of epochs was initially set to 700, early stopping was employed based on validation loss, which typically halted the training after approximately 400 epochs. The early stopping criterion monitored the validation loss with a patience value of 20, meaning training would cease if the validation loss did not improve for 20 consecutive epochs. This ensured that the model did not undergo excessive training, thereby mitigating the risk of overfitting. Regularization techniques, including a 0.5 dropout rate, L2 regularization (weight decay of 0.1), and batch normalization, were also employed, further reinforcing the robustness of the model against overfitting. This was confirmed by consistent performance across 5-fold stratified cross-validation. Key hyperparameters included a kernel length of 250, 8 filters in the first block, a depth multiplier of 16, and 128 filters in the second block. To capture the overall effects of TEAS on EEG signals, we used 5-fold cross-validation, ensuring balanced representation of TEAS frequencies across all splits, with 80% training and 20% testing in each fold. Segments from all participants were included in both the training and test sets, allowing the model to generalize the effects of TEAS on EEG signals. This method provided a comprehensive understanding of TEAS's overall impact on EEG activity without overfitting, as evidenced by the early stopping mechanism and the consistent validation performance across folds. Sensitivity (recall) measures the proportion of actual positives for each class that are correctly identified by the classifier. It is crucial in applications where the omission of a condition can have serious consequences. Sensitivity for class c is calculated as:

$$Sensitivity_c = \frac{TP_c}{TP_c + FN_c} \tag{1}$$

Specificity for a multi-class classification assesses the model's ability to correctly identify instances that do not belong to each particular class. For class c, specificity is calculated as:

$$Specificity_c = \frac{TN_c}{TN_c + FP_c} \tag{2}$$

Precision quantifies the number of correct positive predictions made by the classifier for each class. It is defined for class c as:

$$Precision_c = \frac{TP_c}{TP_c + FP_c} \tag{3}$$

The F1-score is the harmonic mean of precision and sensitivity for each class, providing a single score that balances the two metrics. It is calculated for class c as:

$$F1\text{-}Score_c = 2 \times \frac{Precision_c \times Sensitivity_c}{Precision_c + Sensitivity_c} \tag{4}$$

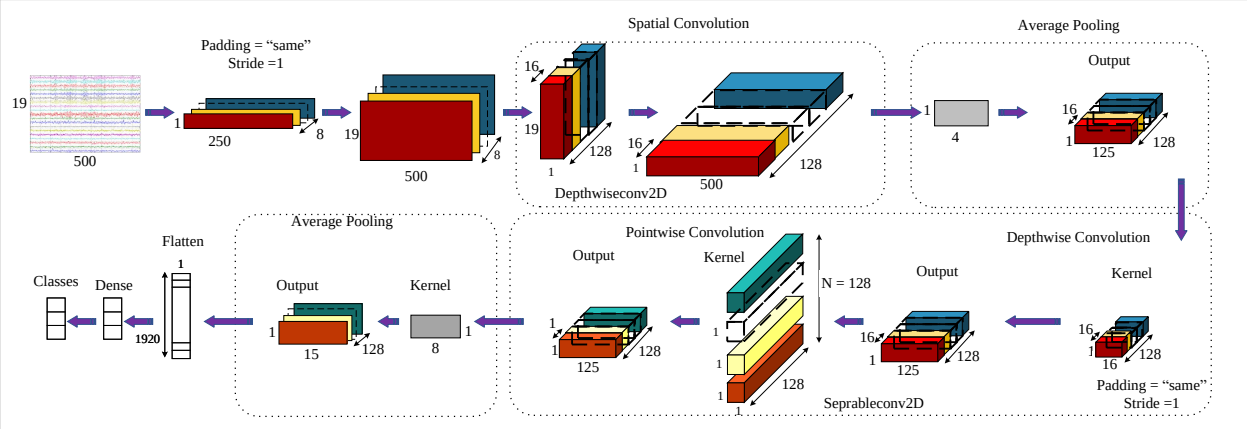

Figure 1. Block diagram of the customized EEGNet architecture.

II-D. Saliency Map Computation

To interpret the decision-making process of our neural network model, we utilized saliency maps to extract the influential features within the EEG data for classification. Saliency maps highlight the sensitivity of the output to changes in the input [16]. We approximated the class score function $S_c(\mathbf{I})$ near the input EEG signal $\mathbf{I}_0$ using the first-order Taylor expansion, computed as:

$$S_c(\mathbf{I}) \approx \mathbf{w}^T \mathbf{I} + b \tag{5}$$

where $\mathbf{W} = \frac{\partial S_c}{\partial \mathbf{I}}\Big|_{\mathbf{I}_0}$ represents the saliency map for class c. These maps were normalized to ensure meaningful interpretation [17]:

$$\mathbf{W}'_c(\mathbf{I}) = \frac{\mathbf{W}_c(\mathbf{I}) - \min(\mathbf{W}_c(\mathbf{I}))}{\max(\mathbf{W}_c(\mathbf{I})) - \min(\mathbf{W}_c(\mathbf{I}))} \tag{6}$$

Aggregated saliency maps were computed for multiple samples to obtain a mean map for each class [18].

II-E. Electrode Importance Scoring

We quantified the importance of each EEG electrode by summing the saliency values across the time dimension, resulting in a single saliency value per electrode for each class:

$$E_{c,k} = \sum_t \bar{\mathbf{W}}_{c,k,t} \tag{7}$$

where $E_{c,k}$ is the summed saliency value for class c at electrode k, and $\bar{\mathbf{W}}_{c,k,t}$ is the mean saliency value at time t for electrode k. These values were normalized to compare the relative importance within the class:

$$E'_{c,k} = \frac{E_{c,k}}{\sum_j E_{c,j}} \tag{8}$$

To determine the overall importance of each electrode across all classes, we aggregated the normalized importance scores:

$$E''_k = \sum_c E'_{c,k} \tag{9}$$

Electrodes were then ranked based on their aggregated importance scores to identify the most influential electrodes in the classification task.

III. Results

III-A. Classification Performance Across TEAS Sessions

Our initial task was to evaluate the variability in brain response to different TEAS frequencies using the EEGNet deep learning model. Table 1 presents the classification accuracy for the four TEAS frequencies (2.5, 10, 80, and sham at 160 pps) across various time slots during stimulation. The results demonstrate that the classification accuracies consistently exceeded 95%, indicating the model's high reliability in correctly identifying the four TEAS frequency classes. Sensitivity was above 93%, specificity over 97%, precision above 94%, and F1-score exceeded 95% for all classes, validating the model's high accuracy in classification tasks. This suggests that TEAS at various frequencies may engage different neural mechanisms and pathways. Understanding these EEG differences can help tailor TEAS treatments to achieve specific therapeutic effects, optimize stimulation protocols for individual patients, and provide a better understanding of how acupuncture influences brain activity in real time.

III-B. Assessing Various TEAS Frequencies in Each Time Slot

Next, we explored how brain activity varied across different phases of TEAS sessions. Table 2 displays the classification accuracies for pre-stimulation, during stimulation, and post-stimulation phases. The results indicate that EEGNet maintained high classification accuracies across all phase for each TEAS frequency, consistently achieving over 95% accuracy. Sensitivity, specificity, precision, and F1 score metrics also displayed high values, indicating robust model performance in differentiating brain activity phases. This

Table 1. Total classification accuracy during the stimulation across different TEAS frequencies. All values are presented as mean accuracies with the overall range of standard deviations being 0.2% to 0.62%. The abbreviations used in the table:Sen: Sensitivity, Spe: Specificity, Pre: Precision, F1: F1 Score.

Slot	Accuracy	2.5 pps				10 pps				80 pps				Sham			
		Sen	Spe	Pre	F1	Sen	Spe	Pre	F1	Sen	Spe	Pre	F1	Sen	Spe	Pre	F1
Slot 2	95.65	0.95	0.98	0.95	0.95	0.96	0.97	0.94	0.95	0.93	0.99	0.98	0.95	0.96	0.97	0.94	0.95
Slot 3	96.70	0.96	0.99	0.97	0.96	0.96	0.98	0.98	0.97	0.97	0.98	0.96	0.97	0.97	0.99	0.95	0.96
Slot 4	96.45	0.96	0.97	0.94	0.95	0.97	0.98	0.96	0.96	0.95	0.98	0.97	0.96	0.95	0.98	0.97	0.96
Slot 5	97.66	0.97	0.99	0.97	0.97	0.98	0.99	0.97	0.97	0.96	0.98	0.97	0.97	0.98	0.99	0.98	0.98

provides a view of how TEAS affects brain activity over time, which may help in better understanding immediate neural responses and the overall dynamic profile of brain activity modulation, contributing to optimizing therapeutic strategies and advancing knowledge of TEAS neurophysiological mechanisms.

III-C. Classification of TEAS Stimulation Phases Across Frequencies

We further assessed classification accuracies during specific stimulation phases (slots 2-5) for different TEAS frequencies. As shown in Table 3, the model maintained high accuracy, consistently exceeding 93% across all frequencies. This finding indicate that TEAS stimulation can induce dynamic changes in EEG signals over time, reflecting the brain's response to the treatment and the progressive relaxation and modulation of brain activity during the stimulation.

III-D. Evaluating EEG Frequency Band Responsiveness to TEAS

We also evaluated the responsiveness of each EEG frequency band of delta (1-4 Hz), theta (4-8 Hz), alpha (8-13 Hz), beta (13-30 Hz), and gamma (30-50 Hz) to TEAS. The classification accuracies were averaged across various EEG frequency bands during different TEAS phases as indicated in Table 2. Figure 2 summarizes the averaged accuracies, revealing that the beta and gamma frequency band exhibited the highest responsiveness, with classification accuracies exceeding 90%. Beta frequency is associated with active thinking, focus, and cognitive processing. changes in beta frequency may indicate that TEAS enhances alertness and cognitive function, possibly by reducing anxiety and stress. Gamma frequency is linked to high-level cognitive functions, such as information processing, memory, and consciousness. Changes in gamma activity could suggest improved neural synchrony and integration of sensory information.

III-E. Optimizing Electrode Selection for EEG-Based TEAS Frequency Classification Using Saliency Maps

To refine the electrode selection for EEG-based classification of TEAS frequencies, we used saliency maps to identify the most significant electrodes. Figure 3 shows the topographic distribution of aggregated saliency maps for various TEAS frequencies. Electrodes Fp1, Fp2, Fz, F7, F8, T3, and T4 were identified as the most influential. Table 4 lists the combinations of these electrodes. Figure 4 illustrates the classification accuracy for incremental electrode combinations, demonstrating that a subset of seven electrodes achieved accuracy close to the full 19-electrode set. This indicates the efficiency of the selected subset, which could streamline EEG protocols and improve patient comfort. We opted to extract saliency maps from a single model, as preliminary experiments demonstrated consistently high classification accuracy across various electrode subsets, confirming the model's robustness. This approach ensured that the saliency maps offered a reliable and generalized interpretation of the brain's response to TEAS. The electrodes Fp1 and Fp2, located over the prefrontal cortex, are critical regions involved in cognitive control, decision-making, and emotional regulation. Previous studies (e.g., [19], [20]) have demonstrated that acupuncture and TEAS modulate prefrontal cortex activity, aligning with our saliency maps that highlight these electrodes. Fz, positioned over the midline frontal cortex, plays a role in motor control and attention, areas that are potentially influenced by TEAS, especially in contexts like pain management or cognitive enhancement. Additionally, T3 and T4, located over the temporal lobes, are involved in auditory processing,

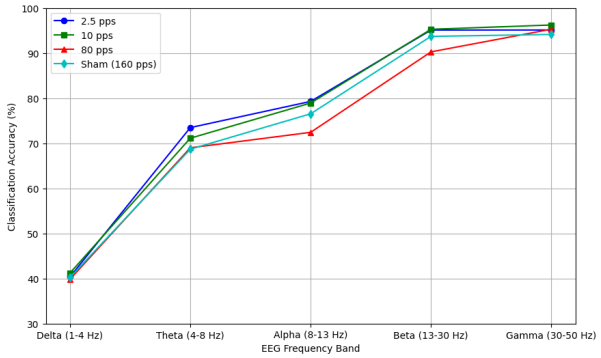

Figure 2. Averaged classification accuracy at each EEG frequency band for different TEAS frequencies across time.

Table 2. Average classification accuracy and metrics for different TEAS frequencies across time slots. All values are presented as mean accuracies with the overall range of standard deviations being 0.18% to 0.70%. The abbreviations used in the table: Sen: Sensitivity, Spe: Specificity, Pre: Precision, F1: F1 Score, Stim: TEAS Stimulation

Frequency	Accuracy	Pre-Stim				Stim				Post-Stim			
		Sen	Spe	Pre	F1	Sen	Spe	Pre	F1	Sen	Spe	Pre	F1
Sham	95.02	0.96	0.97	0.94	0.95	0.94	0.98	0.95	0.95	0.95	0.98	0.95	0.95
10	96.63	0.97	0.98	0.97	0.97	0.96	0.99	0.97	0.97	0.97	0.98	0.96	0.97
2.5	96.53	0.97	0.98	0.96	0.97	0.96	0.99	0.97	0.97	0.96	0.99	0.97	0.97
80	96.12	0.96	0.98	0.96	0.96	0.95	0.98	0.96	0.96	0.96	0.98	0.96	0.96

Table 3. Total classification accuracy during stimulation phase across different TEAS frequencies. All values are presented as mean accuracies with the overall range of standard deviations being 0.18% to 0.60%. The abbreviations used in the table: Sen: Sensitivity, Spe: Specificity, Pre: Precision, F1: F1 Score.

Frequency	Accuracy	Slot 2				Slot 3				Slot 4				Slot 5			
		Sen	Spe	Pre	F1	Sen	Spe	Pre	F1	Sen	Spe	Pre	F1	Sen	Spe	Pre	F1
2.5	95.98	0.97	0.98	0.96	0.96	0.97	0.97	0.94	0.95	0.95	0.99	0.98	0.96	0.95	0.98	0.97	0.96
10	95.68	0.97	0.97	0.93	0.95	0.96	0.99	0.98	0.97	0.93	0.98	0.96	0.95	0.96	0.98	0.96	0.96
80	96.36	0.97	0.98	0.97	0.97	0.96	0.98	0.96	0.96	0.95	0.98	0.96	0.95	0.98	0.99	0.97	0.98
Sham	93.52	0.94	0.98	0.94	0.94	0.91	0.98	0.95	0.93	0.93	0.98	0.94	0.93	0.96	0.96	0.91	0.93

Table 4. Electrode combinations and their corresponding electrode label

Name of Combinations	Name of Electrodes
comb1	Fp1, Fp2
comb2	Fp1, Fp2, Fz
comb3	Fp1, Fp2, Fz, F8, F7
comb4	Fp1, Fp2, Fz, F8, F7, T3, T4
all electrodes	Fp1, Fp2, F7, F3, Fz, F4, F8, T3, C3, Cz, C4, T4, T5, P3, Pz, P4, T6, O1, O2

memory, and emotional regulation. Their inclusion as critical electrodes suggests that TEAS may modulate temporal lobe activity, influencing memory and emotional responses, particularly in cases of chronic pain or stress.

IV. Summary

This paper investigates the neurophysiological effects of TEAS on brain activity using advanced machine learning techniques. We analyzed EEG data from 48 participants subjected to various TEAS frequencies (2.5, 10, 80, and sham at 160 pulses per second) to understand the brain's response. Employing EEGNet, a convolutional neural network optimized for EEG signal processing, we achieved over 93% classification accuracy in 1) differentiating brain responses to different TEAS frequencies at various stimulation slots, 2) detecting the effect of TEAS across the three phases at different TEAS frequencies, and 3) evaluating the dynamic changes of brain responses during stimulation slots at each TEAS frequency. Furthermore, our analysis of individual EEG frequency bands revealed that TEAS induces distinct changes in EEG signals over time, especially in the beta and gamma frequency bands. These changes suggest that TEAS enhances cognitive functions and neural synchrony, leading to reducing anxiety and stress.

Finally, saliency maps identified critical EEG electrodes, revealing that a subset of seven electrodes could achieve classification accuracy close to the full 19-electrode set. This finding suggests the potential for optimizing EEG protocols, reducing the number of electrodes needed without compromising accuracy. Our study advances the understanding of TEAS's neurophysiological mechanisms and demonstrates the efficacy of deep learning models in EEG signal classification. These insights could inform the optimization of TEAS protocols for therapeutic applications, enhancing patient outcomes and providing a deeper understanding of how acupuncture influences brain activity in real time.

References

[1] Y.-T. Kang, Y.-S. Liao, and C.-L. Hsieh, "Different effects of transcutaneous electric nerve stimulation and electroacupuncture at st36–st37 on the cerebral cortex," *Acupuncture in Medicine*, vol. 33, no. 1, pp. 36–41, 2015.

[2] M. Zhang, H. Zhang, P. Li, and J. Li, "Effect of transcutaneous electrical acupoint stimulation on the quality of postoperative recovery: a meta-analysis," *BMC Anesthesiology*, vol. 24, no. 1, p. 104, 2024.

[3] J.-r. Zhang, Y. Ruan, X. Wang, Y.-l. You, Z.-f. Yin, and W. Gu, "Effect of transcutaneous electrical acupoint stimulation on sleep quality: A systematic review and meta-analysis," *European Journal of Integrative Medicine*, p. 102338, 2024.

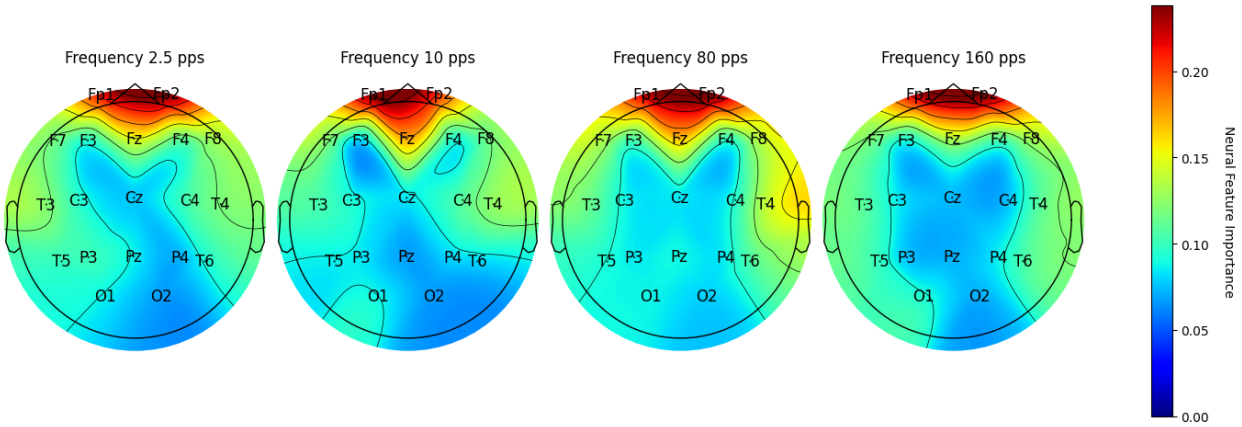

Figure 3. Topographic distribution of aggregated saliency maps for various TEAS frequencies. The color scale indicates the relative importance of each electrode's signal in the model's classification, with warmer colors indicating higher saliency.

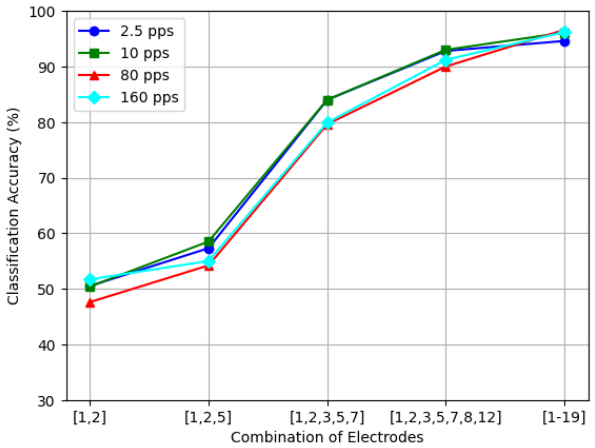

Figure 4. Aggregated classification accuracy of the three phases for incremental electrode combinations.

[4] J. Qin, X. Ye, C. Ye, X. Huang, H. Sun, X. Zhao, Y. Tong, M. Mazomba, and Y. Mo, "The effect of transcutaneous electrical acupoint stimulation on high-risk patients with ponv undergoing laparoscopic gynecologic surgery: a randomized controlled trial," *Journal of Clinical Medicine*, vol. 12, no. 3, p. 1192, 2023.

[5] R. Zhang, L. Lao, K. Ren, and B. M. Berman, "Mechanisms of acupuncture–electroacupuncture on persistent pain," *Anesthesiology*, vol. 120, no. 2, pp. 482–503, 2014.

[6] R. Zhang, L. Lao, K. Ren, and B. M. Berman, "Mechanisms of acupuncture–electroacupuncture on persistent pain," *Anesthesiology*, vol. 120, no. 2, pp. 482–503, 2014.

[7] C. Huang, Y. Wang, J.-S. Han, and Y. Wan, "Characteristics of electroacupuncture-induced analgesia in mice: Variation with strain, frequency, intensity and opioid involvement," *Brain Research*, vol. 945, no. 1, pp. 20–25, 2002.

[8] G. A. Ulett, S. Han, and J.-S. Han, "Electroacupuncture: Mechanisms and clinical application," *Biological Psychiatry*, vol. 44, no. 2, pp. 129–138, 1998.

[9] Ç. Uyulan, D. Mayor, T. Steffert, T. Watson, and D. Banks, "Classification of the central effects of transcutaneous electroacupuncture stimulation (teas) at different frequencies: A deep learning approach using wavelet packet decomposition with an entropy estimator," *Applied Sciences*, vol. 13, no. 4, p. 2703, 2023.

[10] D. Mayor, "An exploratory review of the electroacupuncture literature: clinical applications and endorphin mechanisms," *Acupuncture in Medicine*, vol. 31, no. 4, pp. 409–415, 2013.

[11] T.-W. Lee, M. Girolami, and T. J. Sejnowski, "Independent component analysis using an extended infomax algorithm for mixed subgaussian and supergaussian sources," *Neural Computation*, vol. 11, no. 2, pp. 417–441, 1999.

[12] I. Winkler, S. Haufe, and M. Tangermann, "Automatic classification of artifactual ica-components for artifact removal in eeg signals," *Behavioral and Brain Functions*, vol. 7, pp. 1–15, 2011.

[13] L. Pion-Tonachini, K. Kreutz-Delgado, and S. Makeig, "Iclabel: An automated electroencephalographic independent component classifier, dataset, and website," *NeuroImage*, vol. 198, pp. 181–197, 2019.

[14] J. Kayser and C. E. Tenke, "Principal components analysis of laplacian waveforms as a generic method for identifying erp generator patterns: I. evaluation with auditory oddball tasks," *Clinical Neurophysiology*, vol. 117, no. 2, pp. 348–368, 2006.

[15] V. J. Lawhern, A. J. Solon, N. R. Waytowich, S. M. Gordon, C. P. Hung, and B. J. Lance, "Eegnet: A compact convolutional neural network for eeg-based brain–computer interfaces," *Journal of Neural Engineering*, vol. 15, no. 5, p. 056013, 2018.

[16] K. Simonyan, A. Vedaldi, and A. Zisserman, "Deep inside convolutional networks: Visualising image classification models and saliency maps," *arXiv preprint arXiv:1312.6034*, 2013.

[17] J. Adebayo, J. Gilmer, M. Muelly, I. Goodfellow, M. Hardt, and B. Kim, "Sanity checks for saliency maps," *Advances in Neural Information Processing Systems*, vol. 31, 2018.

[18] D. Erhan, Y. Bengio, A. Courville, and P. Vincent, "Visualizing higher-layer features of a deep network," *University of Montreal*, vol. 1341, 2009, p. 3.

[19] H. Wang, N. Yin, A. Wang, and G. Xu, "Cortical functional networks of transcutaneous electrical stimulation at acupoints on the pericardial meridian," *Neuropsychologia*, vol. 189, 2023, 108669.

[20] S.-p. Kong, Q.-w. Tan, Y. Liu, X.-h. Jing, B. Zhu, Y.-j. Huo, B.-b. Nie, and D.-h. Yang, "Specific correlation between the hegu point (li4) and the orofacial part: evidence from an fmri study," *Evidence-Based Complementary and Alternative Medicine*, vol. 2015, no. 1, 2015, 585493.